

Effects of the N-Methyl-D-Aspartate Hypofunction Model of Schizophrenia Induced By Ketamine on Neuropil of the Hippocampus: A Stereological and Transmission Electron Microscopy Analysis

Original
Article

Shahriar Ahmadpour^{1,2}, Mohammad Amin Forqani², Amir Hossein Najmi², Maedeh Amiri Shahri², Shayan Zanjani² and Mahdi Noori²

¹Neuroscience Education and Research Center (NERC)

²Department of Anatomy, Faculty of Medicine, North Khorasan University of Medical Sciences, Bojurd, Iran

ABSTRACT

Introduction: The neuropil is a dense network between the neuroglial elements and is involved in many activities, such as cognitive functions. Neuropil involvement has been noticed in neurologic disorders. Schizophrenia is a mental health condition defined by a reduction in cognitive functioning. The hippocampus is the key structure of the limbic system regulates cognitive functions.

Aim of the Work: Was to investigate the possible impacts of schizophrenia on the neuropil in the hippocampus.

Material and Methods: Thirty male wistar rats were used in this study. The rats were categorized into three distinct groups (N=10 per group) namely: ketamine, normal saline (1ml, intraperitoneal) (Sham), and control groups. The ketamine group was treated with ketamine (10mg/kg, IP) for seven days. The sham received only Normal saline (1ml, intraperitoneal). After one week the brains were removed and the sections were further processed for histological study. Neuropil surface was measured by stereological method. TEM study was used to study the ultrastructural changes.

Results: In contrast to the sham and control groups, there was a notable increase in the surface areas of CA4, CA3, and CA1 in schizophrenia ($P=0.006$). The number of degenerated neurons in the cornu Ammonis regions showed a remarkable increase ($p=0.001$). Transmission electron microscopy results revealed a wide range of ultrastructural changes including dark neurons, extracellular space disruption, myelin damage, and mitochondrial degeneration in the schizophrenia group.

Conclusion: Schizophrenia leads to neuropil expansion in the CA subregions. The neuropil expansion is associated with ultrastructural changes including mitochondrial degeneration, axonal damage, and neuronal degeneration.

Received: 23 June 2024, **Accepted:** 13 August 2024

Key Words: Hippocampus, neuropil, schizophrenia.

Corresponding Author: Shahriar Ahmadpour, PhD, Neuroscience Education and Research Center (NERC), Department of Anatomy, Faculty of Medicine, North Khorasan University of Medical Sciences, Bojurd, Iran, **Tel.:** +989021232016, **E-mail:** Shahahmadpour@gmail.com

ISSN: 1110-0559, Vol. 48, No. 3

INTRODUCTION

The neuropil is the interwoven network of neuroglial elements that integrates neuronal processing. Structurally, each neuropil is a complex network composed of neuroglial processes and microvascular^[1]. Recent data revealed that the neuropil contributes to a wide range of neurodevelopmental and functional activities including neuronal plasticity and cortical gyrification^[2,3]. Considering the critical role of the neuropil in neuronal processing, researchers have turned their attention to the neuropil in the pathophysiology of neuropsychiatric disorders. Interestingly, many studies have yielded conclusive proof indicating the neuropil role(s) in central nervous system disorders^[4]. One of the debilitating psychiatric disorders is schizophrenia. It is known as a severe mental illness characterized by psychosis, hallucination, thought

disorders, and progressive cognitive deficits^[5]. Although schizophrenia has been known as a psychiatric disorder, it should bear in mind that schizophrenia is an umbrella term for a wide spectrum of symptoms. Due to its multifactorial etiology and multifaceted presentation, its underlying mechanism(s) has not been fully understood^[6]. In recent decades, researchers have turned their attention toward the possible anatomic substrate involved in the declined cognitive performance in schizophrenia. Accordingly, pathologic alterations have been demonstrated in the structures connected to mental and emotional processing in both experimental and postmortem studies^[7-11]. One of the key areas that is essential to learning, memory processing, and cognitive performance is the hippocampus^[12]. Interestingly, hippocampus involvement has been known as the hallmark of schizophrenia^[13]. Recent studies have

provided evidence suggesting the disturbances between the structural connectivity of the hippocampus and cortical/subcortical structures^[14,15].

Structurally, the hippocampus comprises the cornu Ammonis and the dentate gyrus^[16]. Cornu Ammonis is subdivided into four regions CA1-CA4 which is thought to be the primary target of the neurodegenerative process^[17]. Given the lack of data on the effects of schizophrenia on the neuropil in the hippocampus and discrepancies in the few previous reports, this study was done to investigate the neuropil in the cornu Ammonis in schizophrenia by quantitative and transmission electron microscopy analysis.

MATERIALS AND METHODS

In this research, thirty mature male wistar rats (weighing 200±20g) were utilized. The NKUMS ethics committee approved the research protocols for biomedical research (Ethical code: IR.NKUMS.REC.1402.057). The rats were randomly assigned to three groups (N=10) namely, ketamine(experiment), Normal saline (NS, Sham), and control. The experimental group was treated with ketamine (10mg/kg, intraperitoneally) for seven consecutive days^[18]. The sham group received saline (1ml, intraperitoneally, seven days). At the end of the first week, under deep anesthesia, the chest was opened and the heart was exposed. Subsequently, 100 ml of buffered formalin and heparin were perfused through the left ventricle^[19]. To remove the brain, a sagittal incision was made through the skin and the cranium vault opened. The removed samples were processed as per the reported protocol and stained with cresyl violet (MP Biomedicals, France)^[20]. The cornu Ammonis subregions were defined under low magnification and photographs were taken under X100 magnification. The pictures from the selected fields were processed by Image J software. Quantitative analysis was performed by stereological frame (159 µm ×355 µm) superimposed on each photo. The neuropil area and the number of degenerated neurons were measured in each randomized field^[4,21].

Transmission Electron Microscopy (TEM)

The hippocampus samples were processed as previous study^[22]. To identify the cornu Ammonis, semithin sections of epoxy-resin embedded samples were obtained and stained with 1% toluidine blue. Finally, lead citrate and uranyl acetate were used to stain the thin sectioning (60–90 nm). An EM900(Zeiss, Germany) was used to conduct ultrastructural analysis.

Statistical Analysis

The results were entered into SPSS (version 13). Statistical significance was set to $p<0.05$. In order to compare the results between groups we used one-way analysis of variance (ANOVA) and post-hoc Tukey test.

RESULTS

Descriptive histology

CA4 region: pyramidal neurons with prominent nuclei and defined margins and scattered astrocytes and oligodendrocytes were the characteristic features in the control group (Figure 1). Large pyramidal neurons with scattered astrocytes were observed in the NS group. (Figure 2). The main microscopic features in the ketamine group were degenerating dark neurons with dense and hyperchromatic appearance, oligodendrocytes, and astrocytes (Figure 3).

CA3 Region: The control group's primary findings were pyramidal neurons with scattered astrocytes (Figure 4), while the sham group's main findings were a few degenerated neurons and astrocytes (Figure 5). The CA3 region in the ketamine group presented dark and degenerating neurons, vacuolization, and hypertrophic astrocytes (Figure 6).

CA1 region: closely packed healthy neurons with prominent nuclei were observed in control (Figure7) and Normal saline groups (Figure 8) while in the ketamine group hyperchromatic and shrunk neurons were noticed among the healthy-looking neurons (Figure 9). Oligodendrocytes and astrocytes around the neurons and disrupted extracellular matrix were remarkable microscopic features in the ketamine group (Figure 9).

Quantitative results

The neuropil surface fraction in the CA4, CA3, and CA1 regions displayed a considerable increase in the schizophrenia group when set beside those of the control and saline(sham) groups (Figure 10 A,B,C, Table 1). Increased neuropil surface area was also noticed in the CA3 and CA1 regions in the sham group. Interestingly the CA4 region of the sham group showed a meaningful decrease.

The rate of neurodegeneration in the schizophrenia group(ketamine-treated) showed a remarkable increase when compared to the NS and control groups (Table 2). Additionally, comparing the counted degenerated neurons in the CAs region in the ketamine-treated animals showed meaningful differences (Table 2).

TEM Results

Neurons with light nuclei and oligodendrocytes with typical dark nuclei and cytoplasm close to neurons were noticed in the control group (Figure 11). A few degenerated dark neurons with electron-dense appearance, oligodendrocyte, and vacuolized ECM were seen in the NS group (Figure 12). In the ketamine group, a wide range of pathology was observed. A considerable number of dark neurons with disrupted extracellular space and the presence of astrocytes (Figures13,14) degenerated dendrite (Figure 15), oligodendrocytes in the vicinity of degenerated neurons (Figure 16), myelin sheath damage, and mitochondrial degeneration (Figure17) were the striking features in the ketamine group.

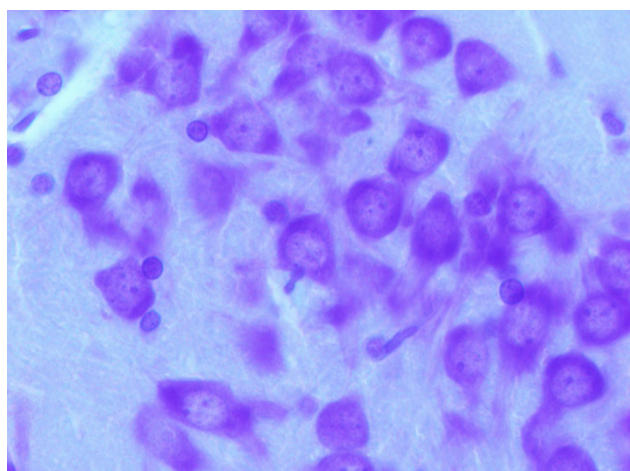


Fig. 1: CA4 control. Healthy neurons (red arrowheads) and oligodendrocytes close to neurons (yellow arrowheads) are seen. Cresyl violet staining.X100

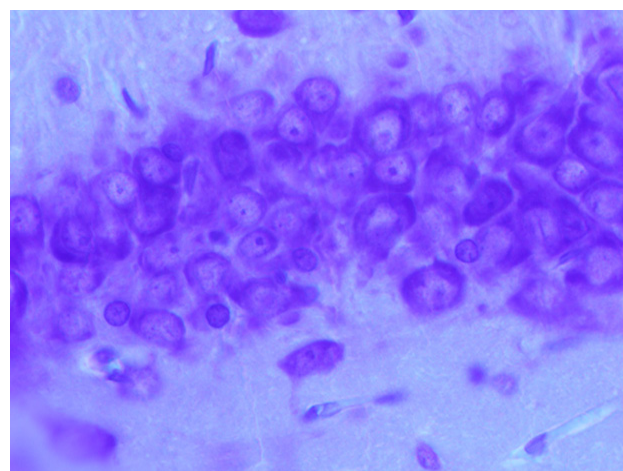


Fig. 4: CA3 control. Densely packed neurons with prominent nuclei (red arrowheads) and oligodendrocytes (yellow arrowheads) close to the neurons are seen. Cresyl violet staining .X100

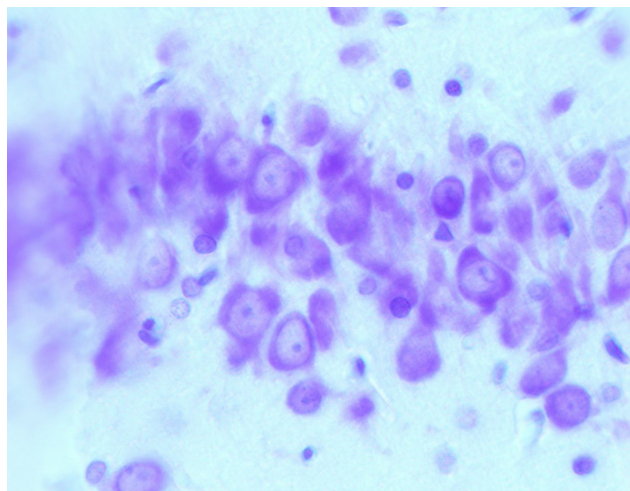


Fig. 2: CA4 region. Normal saline group. Scattered astrocytes with round and light nuclei (black arrowheads) are seen between the neurons (red arrowheads). An oligodendrocyte with triangular and dense chromatin is seen. Cresyl violet staining .X100

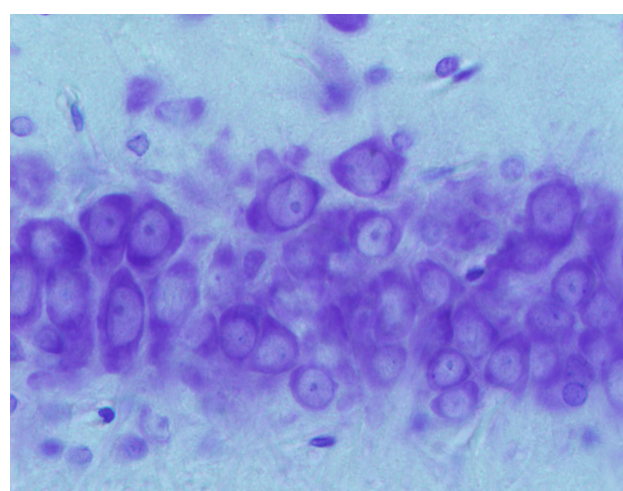


Fig. 5: CA3 Normal saline. Normal neurons (red arrowheads) and oligodendrocytes (black arrowheads). A degenerated neuron with a hyperdense appearance is seen (yellow arrowheads) . Cresyl violet staining .X100

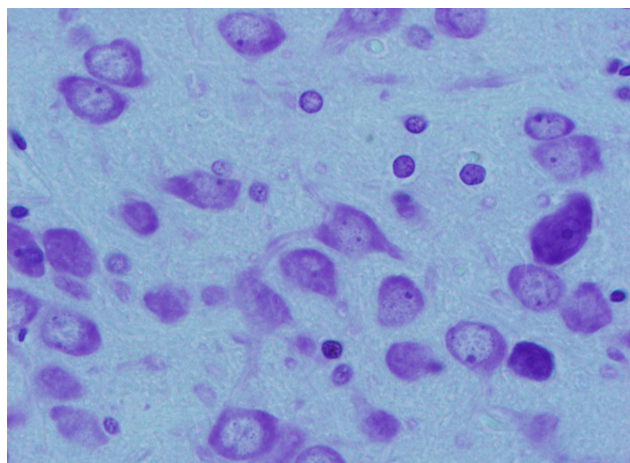


Fig. 3: CA4 ketamine. Dark neurons (red arrowheads) are seen close to the healthy-looking neurons (red arrows) on the right side. Oligodendrocytes (yellow arrows) adjacent to neurons. Scattered astrocytes (yellow arrowheads). Cresyl violet staining.X100

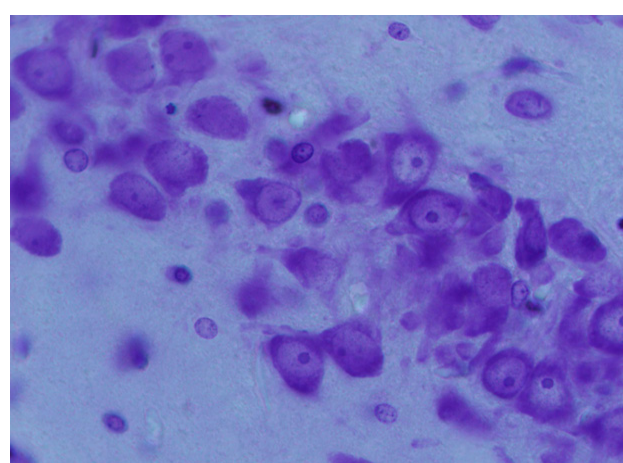


Fig. 6: CA3 ketamine. DNs (red arrows) with dense and hyperchromatic appearance. Astrocytes (yellow arrowheads). Pyknotic neurons (yellow arrow). Vacuolization is also seen (black arrow). Cresyl violet staining .X100

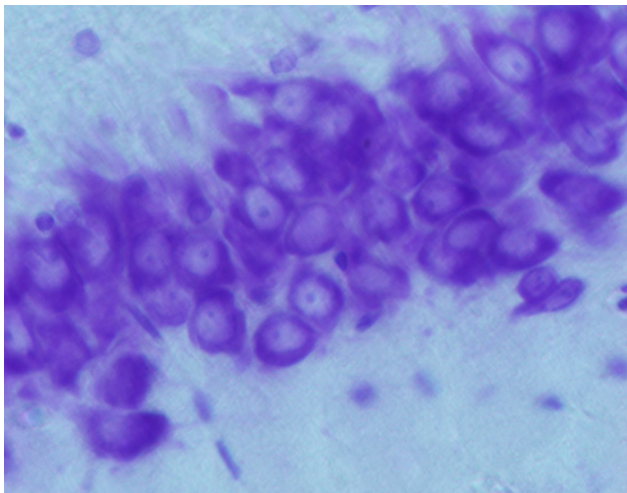


Fig. 7: CA1 control. Healthy-looking neurons with defined nuclei (red arrows). Cresyl violet staining. X100

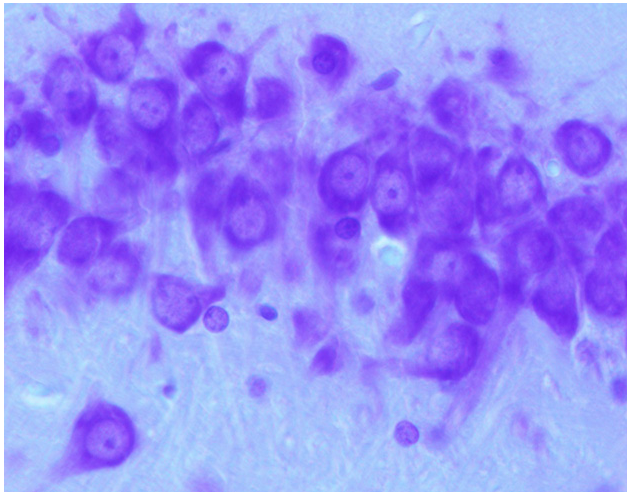


Fig. 8: CA1 Normal saline. Astrocytes (yellow arrowhead) and near (red arrowhead) a neuron Healthy-looking neuron (white arrowheads). Degenerating neurons (black arrowheads) are seen among the normal neurons. X100

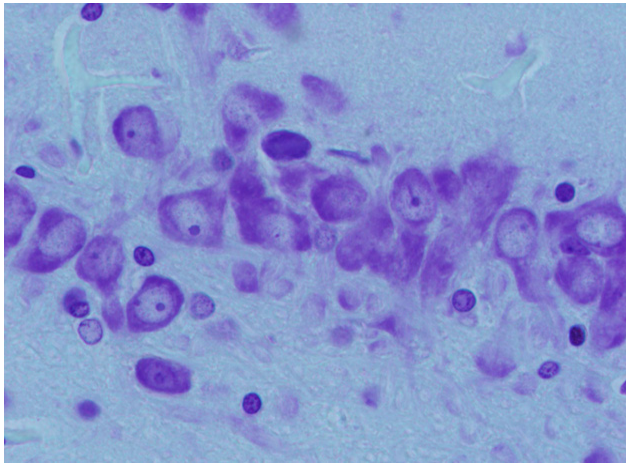


Fig. 9: CA1 ketamine. Astrocytes (yellow arrowheads). DNs are characterized by hyperchromatic and dense appearance (red arrowheads). Astrocytes with light chromatin (yellow arrowhead) and oligodendrocytes (white arrowhead) are seen near the neurons. Cresyl violet staining. X100

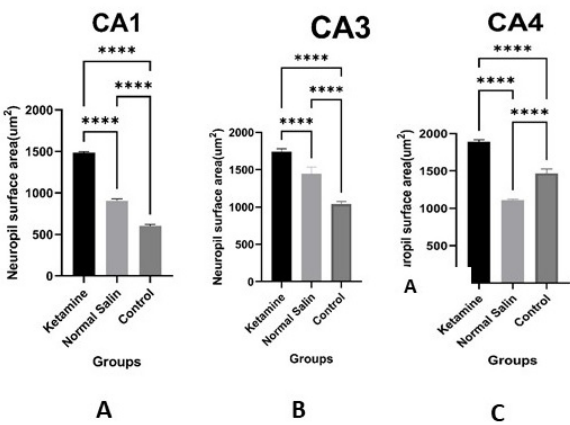


Fig. 10: The Neuropil surface area of the cornu Ammonis in the ketamine group showed meaningful difference in comparison with the normal saline and control groups($p=0.006$)****

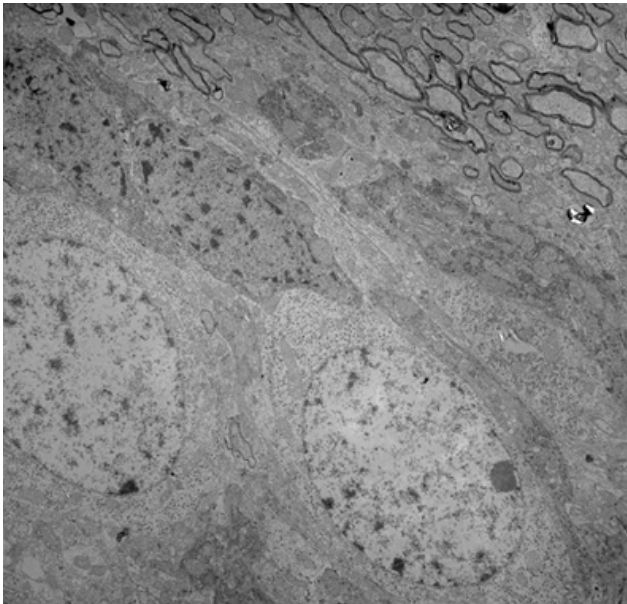


Fig. 11: TEM control. Two oligodendrocytes with oval nuclei and dark cytoplasm (red arrowheads) are seen near neurons (yellow arrowheads). (TEMX3000)

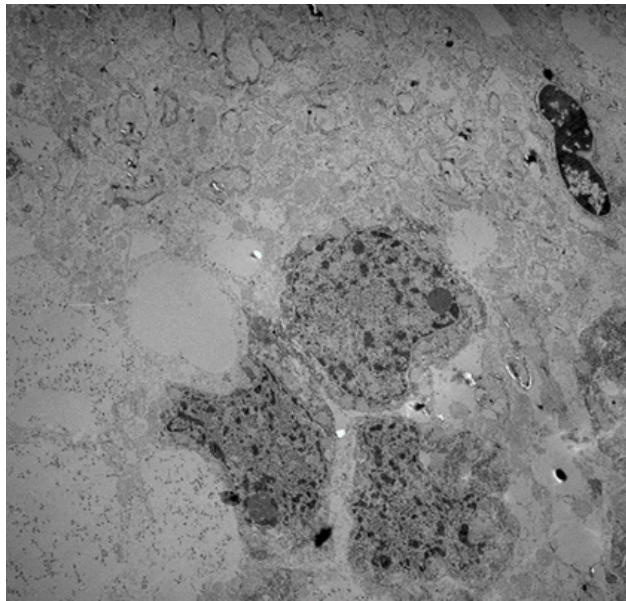


Fig. 12: Normal saline group. Three DNs with electron dense and ruffled outline (red arrowhead). Vacuolization is seen around the DN (yellow arrowhead). Oligodendrocyte presents at right upper corner (blue arrowhead). (TEMX3000)

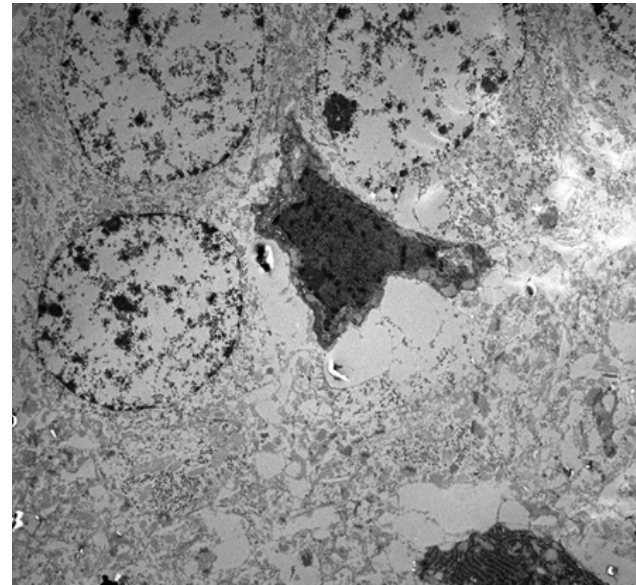


Fig. 14: Ketamine group. DNs with electron-dense appearance (center and right corner) (yellow arrowhead) in the disrupted extracellular space (red asterisks). Astrocytes with light and round nuclei are seen adjacent to DN (red arrowheads). (TEMX3000)

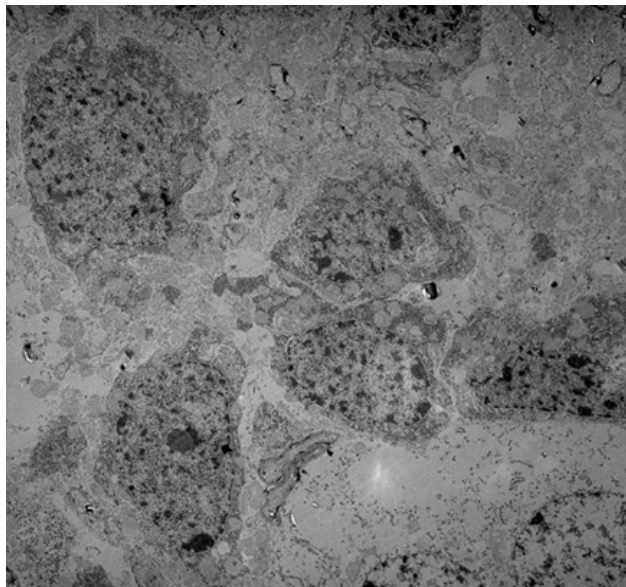


Fig. 13: Ketamine group. DNs with electron-dense appearance (red arrowheads). DNs with preserved integrity, chromatin clumping, and ruffled outlines are seen in the disrupted extracellular space (red asterisks). A degenerating dendrite is noticed (yellow arrowhead). In the lower right corner two astrocytes are seen (blue arrowhead). (TEMX3000)

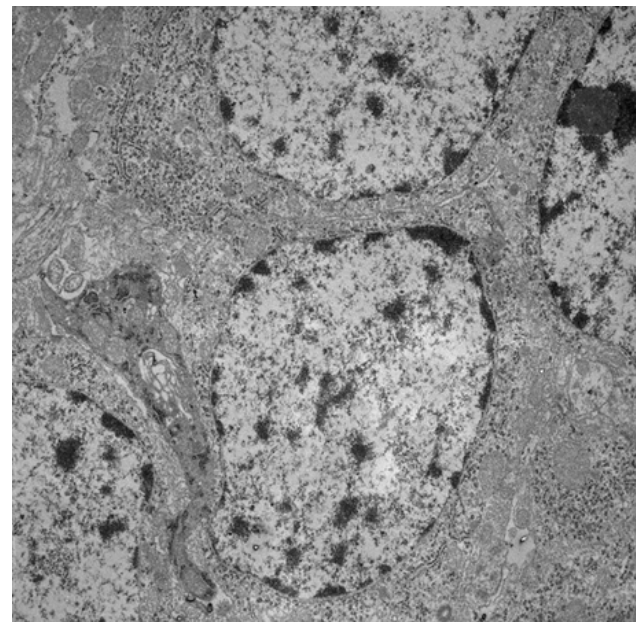


Fig. 15: Ketamine group. DNs with an electron-dense appearance (red asterisk) and a degenerated dendrite (yellow arrowhead) are seen. (TEMX5000)

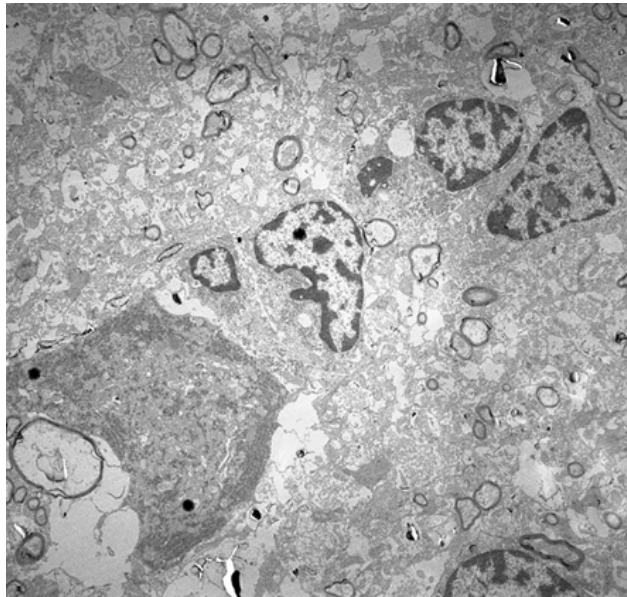


Fig. 16: Ketamine group. DNs with an electron-dense appearance (purple star) are seen in the disrupted extracellular space (red star). Oligodendrocytes with typical heterochromatin are seen in ECM (yellow arrowheads). (TEMX5000)

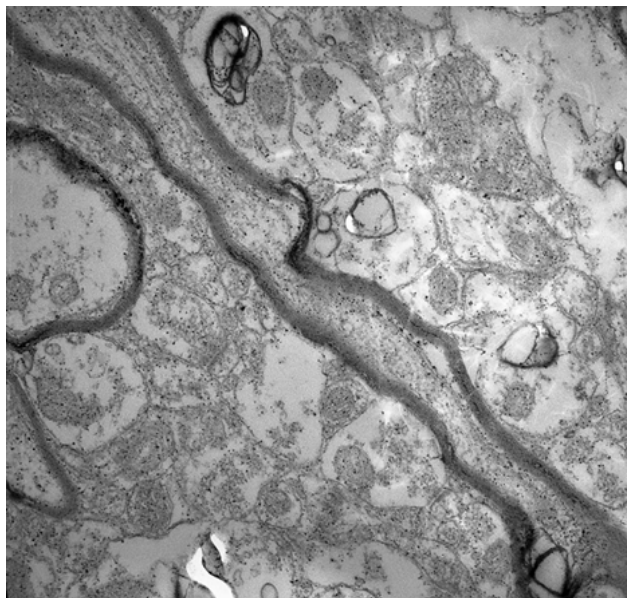


Fig. 17: TEM ketamine. Degenerated dendrites with mitochondria (yellow and red arrowheads). Myelin sheath damage (red star and blue arrowheads) are seen. (TEMX5000)

Table1: The neuropil's surface area was measured in cornu Ammonis. The measured surface area of the ketamine group (Ket) showed a meaningful difference from those of the control (Con) and normal saline (NS) groups ($P=0.006$)*, #

Group	CA4	CA3	CA1
Con	1469.6±53*	1041.1±30.31#	600.9±17.71*
NS	1108.3±12.88**	1449.8±79.42##	905.6±21.49**
Ket	1892±23.27***	1739.6±37.21###	1487.5±10.43***

Table 2: The mean number of counted DNs. The difference between the DNs in the ketamine group (ket) showed a significant level of difference in comparison with the control (Con) and normal saline (NS) groups ($p=0.000$)*

Group	CA4	CA3	CA1
Con	0	<1	<1
NS	<1	<2	<2
Ket	7±1*	8±2*	6±1*

DISCUSSION

Neuropils could be considered microprocessors within the CNS that have been suggested to be involved actively in neuronal processing and plasticity^[1,2]. It is composed of a complex network between the neuroglial elements and synapses. Considering its dynamic nature, neuropil alteration may stem from the perturbed neuro-glial interaction^[4]. At the light microscopic level neuropil is defined as the space between neurons and glial^[4]. The present study used cresyl violet, TEM, and stereology methods to address the neuropil alteration in the cornu Ammonis in schizophrenia. The findings of our research indicated that schizophrenia is linked to an increase in neuropil area in the cornu Ammonis. The TEM results revealed that ketamine- induce schizophrenia leads DNs formation, glial reaction (astrocytes and oligodendrocytes), ECM disruption, and vacuolization. Furthermore, the dominant histological feature of cell death was dense hyperchromatic neurons in the cornu Ammonis. Interestingly, in the Normal saline group neuropil surface area showed an expansion, particularly in the CA3 and CA1 regions, but in the CA4 region neuropil was reduced. These results may be partially explained by the effects of stress due to the injection and regional differences between CA4 and other regions^[23,24]. Comparing the results between the ketamine and Normal saline groups, showed that the neuropil alteration occurred considerably more extensively in the ketamine group, and these results might be attributed to the rate of neurodegeneration and glial reaction. These results have not previously been described and for as much as we know, few studies address the neuropil alteration in schizophrenia. For instance, neuropil contraction in the CA4 has been reported by Prasad *et al*^[25,26]. Parker *et al* also studied the auditory cortex in schizophrenia. The results of their study revealed morphological changes in dendritic spine density and concluded schizophrenia is associated with reduced neuropil area^[26]. They also did not report neuronal loss in the auditory cortex in schizophrenia^[27], while neurodegeneration was one of the striking microscopic features in the ketamine group. These discrepancies may account for methodologic and regional differences in the studied regions^[21]. In the present study, we used histologic and ultrastructure methods to elucidate the possible pathologic alterations. Besides, applying the stereological method allows us to quantify precisely the biological parameters in the samples^[28]. As discussed earlier, the neuropil is defined as a geometry composed of

neuroglial processes and ECM. One of the ultrastructure findings was the vacuolization of the space between the neurons. TEM results could also provide evidence indicating the ECM disruption. In this regard, our findings are consistent with reported data on ECM alterations in schizophrenia^[29,30]. Therefore, it would seem that concomitant neurodegeneration and ECM degradation lead to the structural alteration of neuropil space or geometry. In other words, under the N-Methyl-D-Aspartate (NMDA) hypofunction model of schizophrenia neuropil-defined functional structure undergoes a pathologic reorganization that may impede normal neuronal processing. The morphology of neurodegeneration showed a distinct form of neuronal death as dark neurons (DN). DN is characterized by chromatin clumping with an electrodense appearance, preserved cell membrane, and ruffled outline^[22]. Some may argue the essence of DNs. However, experimental studies have yielded evidence that supports the notion that DN formation is a mode of neuronal death with a reversible nature. During the DN formation, a massive amount of water exits from the neurons which may lead to a change in ECM dimension. The presence of DNs has been documented in stress, pathometabolic, and neurologic disorders like Alzheimer's disease^[31]. Admittedly, DNs identification according to light microscopy and cresyl violet staining could not provide clear-cut evidence and specific staining is required to identify DNs. The results of TEM highlighted DN formation in the NMDA hypofunction model of schizophrenia. Furthermore, mitochondrial damage particularly in dendrites, axonal degeneration, and myelin damage were striking features in the ketamine group. Mitochondrial damage has been known to impact the function of neurons and its dysfunction has been implicated in many neurodegenerative disorders^[32]. Mitochondria functions including ATP production and calcium buffering are pivotal to synaptic activities^[33]. In this regard, a post-mortem study has yielded results suggesting the role of mitochondrial anomalies in schizophrenia^[34]. Recent data have also highlighted the malfunction(s) of mitochondria in schizophrenia^[35]. Our findings are compatible with the previous reports on the alteration of mitochondrial function in schizophrenia. Therefore, this result may support the notion that mitochondria alteration resulting from NMDA hypofunction triggers neurodegeneration in the hippocampus and leads to cognitive impairments^[36]. Now, a question may be raised that considering the results of the ketamine group, neuropil expansion could result from stress or escalating levels of glutamate due to ketamine. Comparing the results between ketamine and Normal saline groups, it would be tenable to assume neuropil expansion in the ketamine group might be at least in part due to accelerated neurodegeneration (DNs). It is worth mentioning that stress could induce neuropil degeneration^[37]. The detrimental effects of stress have been documented thoroughly. In this connection, a plethora of literature documented evidence suggesting the effects of stress on neuronal morphology. For instance, chronic stress

is associated with reversible morphological changes in the dendritic tree^[38]. So, the neuropil alteration in the Normal saline group might at least in part be explained by morphological changes which is an adaptive and reversible phenomenon^[31]. Although, the neuropil in the CA3 and CA1 regions showed an increase in the ketamine and NS groups, comparing the results suggests the accelerated neuropil alteration in the animal model schizophrenia. Consequently, CA4 might be seen as a key region that responds to stress and schizophrenia in two different ways. In this regard, a recent study could provide evidence that suggests the critical role of this region in schizophrenia^[39]. Accordingly, Falaki *et al* showed that disturbed oligodendroglial maturation in CA4 may lead to cognitive dysfunction in schizophrenia. Oligodendrocytes generate myelin in CNS and regulate axonal metabolism^[40]. Oligodendrocytes are extremely sensitive to excitotoxicity. Our results revealed that the NMDA model of hypofunction is associated with neurodegeneration and the presence of oligodendrocytes, which may reflect the myelin damage. The neurotoxic effects of ketamine have been shown in several studies. It has been suggested ketamine neurotoxicity mediates through various complex mechanisms including disturbance in calcium signaling, increased free radical generation, and impaired mitochondrial function which finally leads to neurodegeneration^[41]. It has been demonstrated that ketamine exposure leads to increased levels of glutamate at synaptic space-subsequently, high levels of glutamate result in excitotoxicity and neuronal death. Resultantly, these events may lead to altered synaptic geometry. In other words, neuropil expansion may impede the electrophysiological state (e.g. Gibbs free energy) and trigger neurodegeneration^[42]. Admittedly, schizophrenia is a multifaceted psychiatric disorder and animal models only mimic some aspects of the disorder. On the other hand, in recent years studies have provided evidence supporting the notion that synapse pathologies may be at the core of cognitive disturbance in schizophrenic patients. For this reason, researchers have focused on the synapse alterations in schizophrenia^[43]. Therefore, the elements involved in synapse and synaptic geometry have been revolutionized and a new concept has emerged. The new concept suggests a tetrapartite synapse in which pre and postsynaptic neurons, glial, and ECM are considered the main players of the synapse geometry^[44,45]. Here, we propose a model of the neuropil expansion based on the tetrapartite synapse. Considering our results, neurodegeneration (DNs in this case) and altered ECM would lead to the disintegration of neuropil geometry. Given this, ECM disruption and neurodegeneration compromise the neuropil dimension and integrity. Altered synaptic geometry may interfere with neurotransmitter bioavailability, volume transmission, and neuronal processing^[45]. The proposed model has been suggested to explain the possible mechanisms governing neuropil alteration, certainly, more experimental studies need to elucidate the details of neuropil dynamic in schizophrenia. Considering the nature of the

neurodegeneration, it would seem neuronal loss and subsequent changes in the ECM and glial cells lead to profound alteration of the neuropil geometry in all subregions of cornu Ammonis. Given the results of this study, the magnitude of neurodegeneration, the mode of neuronal loss, and the extent of regional involvement could be considered the main leading factors in neuropil expansion. In conclusion: the animal model of schizophrenia is associated with expanded neuropil geometry in the cornu Ammonis. At the ultrastructural levels, multiple neurodegenerative processes mediate the neuropil-altered dimensions. Accordingly, the altered complex geometry of neuropil may be at the core of abnormal neuronal processing and cognitive impairment as seen in schizophrenia. To sum up, it is recommended to apply the “altered neuropil geometry” term to show the permanent degenerative changes in the neuropil structure in schizophrenia.

CONCLUSION

Schizophrenia leads to neuropil expansion in the CA subregions. The neuropil expansion is associated with ultrastructural changes including mitochondrial degeneration, axonal damage, and neuronal degeneration.

CONFLICT OF INTERESTS

There are no conflicts of interest.

REFERENCES

1. Moyle MW, Barnes KM, Kuchroo M. *et al.* Structural and developmental principles of neuropil assembly in *C. elegans*. *Nature*. (2021);591, 99–104. <https://doi.org/10.1038/s41586-020-03169-5>
2. Baldwin KT, Tan CX, Strader ST, Jiang C, Savage JT, Elorza-Vidal X, Contreras X, Rülcke T, Hippenmeyer S, Estévez R, Ji RR, Eroglu C. HepaCAM controls astrocyte self-organization and coupling. *Neuron*. (2021) Aug 4;109(15):2427–2442.e10. doi: 10.1016/j.neuron.2021.05.025. Epub 2021 Jun 24. PMID: 34171291; PMCID: PMC8547372.
3. Rash BG, Arellano JI, Duque A, Rakic P. Role of intracortical neuropil growth in the gyrification of the primate cerebral cortex. *Proc Natl Acad Sci U S A*. (2023) Jan 3;120(1):e2210967120. doi: 10.1073/pnas.2210967120. Epub 2022 Dec 27. PMID: 36574666; PMCID: PMC9910595.
4. Spocter MA, Fairbanks J, Locey L, Nguyen A, Bitterman K, Dunn R, Sherwood CC, Geletta S, Dell LA, Patzke N, Manger PR. Neuropil Distribution in the Anterior Cingulate and Occipital Cortex of Artiodactyls. *Anat Rec (Hoboken)*. (2018); Nov;301(11):1871–1881. doi: 10.1002/ar.23905. Epub 2018 Oct 5. PMID: 30289208
5. Tandon R, Gaebel W, Barch DM, Bustillo J, Gur RE, Heckers S, Malaspina D, Owen MJ, Schultz S, Tsuang M, Van Os J, Carpenter W. Definition and description of schizophrenia in the DSM-5. *Schizophr Res*. (2013) Oct;150(1):3–10. doi: 10.1016/j.schres.2013.05.028. Epub 2013 Jun 22. PMID: 23800613.
6. McCutcheon RA, Reis Marques T, Howes OD. Schizophrenia-An Overview. *JAMA Psychiatry*. (2020) Feb 1;77(2):201–210. doi: 10.1001/jamapsychiatry.2019.3360. PMID: 31664453.
7. Keshavan MS, Collin G, Guimond S, Kelly S, Prasad KM, Lizano P. Neuroimaging in Schizophrenia. *Neuroimaging Clin N Am*. (2020) Feb;30(1):73–83. doi: 10.1016/j.nic.2019.09.007. Epub 2019 Nov 11. PMID: 31759574; PMCID: PMC7724147.
8. Saarinen AIL, Huhtaniska S, Pudas J, Björnholm L, Jukuri T, Tohka J, Granö N, Barnett JH, Kiviniemi V, Veijola J, Hintsanen M, Lieslehto J. Structural and functional alterations in the brain gray matter among first-degree relatives of schizophrenia patients: A multimodal meta-analysis of fMRI and VBM studies. *Schizophr Res*. (2020) Feb;216:14–23. doi: 10.1016/j.schres.2019.12.023. Epub 2020 Jan 7. PMID: 31924374.
9. Gebreegziabhere Y, Habatmu K, Mihretu A, Cella M, Alem A. Cognitive impairment in people with schizophrenia: an umbrella review. *Eur Arch Psychiatry Clin Neurosci*. (2022) Oct;272(7):1139–1155. doi: 10.1007/s00406-022-01416-6. Epub 2022 May 28. PMID: 35633394; PMCID: PMC9508017.
10. Saint-Georges Z, MacDonald J, Al-Khalili R, et al. Cholinergic system in schizophrenia: A systematic review and meta-analysis. *Mol Psychiatry*. 2025;30(7):3301–3315. doi:10.1038/s41380-025-03023-y
11. Zielinski MC, Tang W, Jadhav SP. The role of replay and theta sequences in mediating hippocampal-prefrontal interactions for memory and cognition. *Hippocampus*. (2020) Jan;30(1):60–72. doi: 10.1002/hipo.22821. Epub 2018 Jan 11. PMID: 29251801; PMCID: PMC6005707.
12. El-Beltagi, E., ElKaliny, H., Moustafa, K., Soliman, G., Zamzam, A. Effect of Bone Marrow-Derived Mesenchymal Stem Cells on the Hippocampal CA1 Area of Aluminium Chloride-Induced Alzheimer's Disease in Adult Male Albino Rat: A Histological and Immunohistochemical Study. *Egyptian Journal of Histology*. (2022); 45(4): 968–985. doi: 10.21608/ejh.2021.78406.1495
13. Liu G, Yu Q, Tan B, Ke X, Zhang C, Li H, Zhang T, Lu Y. Gut dysbiosis impairs hippocampal plasticity and behaviors by remodeling serum metabolome. *Gut Microbes*. (2022) Jan-Dec;14(1):2104089. doi: 10.1080/19490976.2022.2104089. PMID: 35876011; PMCID: PMC9327780.

14. Stanley JA, Daugherty AM, Richter Gorey C, Thomas P, Khatib D, Chowdury A, Rajan U, Haddad L, Amirsadri A, Diwadkar VA. Basal glutamate in the hippocampus and the dorsolateral prefrontal cortex in schizophrenia: Relationships to cognitive proficiency investigated with structural equation modelling. *World J Biol Psychiatry*. (2023) Oct;24(8):730-740. doi: 10.1080/15622975.2023.2197653. Epub 2023 Apr 24. PMID: 36999359; PMCID: PMC10591941.
15. Alves IS, Coutinho AMN, Vieira APF, Rocha BP, Passos UL, Gonçalves VT, Silva PDS, Zhan MX, Pinho PC, Delgado DS, Docema MFL, Lee HW, Policeni BA, Leite CC, Martin MGM, Amancio CT. Imaging Aspects of the Hippocampus. *Radiographics*. (2022) May-Jun;42(3):822-840. doi: 10.1148/rg.210153. Epub 2022 Feb 25. PMID: 35213261.
16. Li H, Jia X, Qi Z, Fan X, Ma T, Pang R, Ni H, Li C-sR, Lu J and Li K .Disrupted Functional Connectivity of Cornu Ammonis Subregions in Amnesic Mild Cognitive Impairment: A Longitudinal Resting-State fMRI Study. *Front. Hum. Neurosci*. (2018) 12:413. doi: 10.3389/fnhum.2018.00413
17. Proescholdt M, Heimann A, Kempfski O. Neuroprotection of S(+) ketamine isomer in global forebrain ischemia. *Brain Res*. (2001); Jun ;22;904(2):245-51. doi: 10.1016/s0006-8993(01)02465-9. PMID: 11406122.
18. Wu J, Cai Y, Wu X, Ying Y, Tai Y, He M. Transcardiac Perfusion of the Mouse for Brain Tissue Dissection and Fixation. *Bio Protoc*. (2021); Mar; 5;11(5):e3988. doi: 10.21769/BioProtoc.3988. PMID: 33796622; PMCID: PMC8005872
19. Ahmadpour S, Chronic exposure to ketamine induces neuronal loss and glial reaction in CA4 region of hippocampus *J. Morphol. Sci.* , 2016, vol. 33, no. 2, p. 103-107
20. Ahmadpour, S. Neuropil Alteration of the Habenula Nucleus in the Experimental Model of Schizophrenia Induced by Ketamine. *IJSRD*, (2023). 5(3), 111-116. doi: 10.30485/ijsrdms.2023.406519.1512
21. Ahmadpour Sh., Haghir H.Diabetes mellitus type1 induces dark neuron formation in the dentate gyrus: A study by Gallyas' method and Transmission Electron Microscopy. *Rom J Morphol Embryol*(2011);52(2):575–579.
22. Abdel Rahman, M., Mohamed, H., Amer, S. The Possible Neuroprotective Role of Selenium in Arsenic-Induced Midbrain Substantia Nigra Neurotoxicity in Guinea Pig Model: Biochemical and Histological Study. *Egyptian Journal of Histology*, 2024; 47(2): 781-791. doi: 10.21608/ejh.2023.189925.1847
23. Chan-Palay V. Quantitative visualization of gamma-aminobutyric acid receptors in hippocampus and area dentata demonstrated by [3H]muscimol autoradiography. *Proc Natl Acad Sci U S A*. (1978) May;75(5):2516-20. doi: 10.1073/pnas.75.5.2516. PMID: 209469; PMCID: PMC392585.
24. Prasad KM, Burgess AM, Keshavan MS, Nimgaonkar VL, Stanley JA. Neuropil pruning in Early-Course Schizophrenia: Immunological, Clinical, and Neurocognitive Correlates. *Biol Psychiatry Cogn Neurosci Neuroimaging*.(2016); Nov;1(6):528-538. doi: 10.1016/j.bpsc.2016.08.007. PMID: 28255578; PMCID: PMC5328666
25. Prasad KM, Burgess AM, Keshavan MS, Nimgaonkar VL, Stanley JA. Neuropil pruning in Early-Course Schizophrenia: Immunological, Clinical, and Neurocognitive Correlates. *Biol Psychiatry Cogn Neurosci Neuroimaging*. (2016); Nov;1(6):528-538. doi: 10.1016/j.bpsc.2016.08.007. PMID: 28255578; PMCID: PMC5328666.
26. Parker EM, Sweet RA. Stereological Assessments of Neuronal Pathology in Auditory Cortex in Schizophrenia. *Front Neuroanat*. (2018) Jan 9;11:131. doi: 10.3389/fnana.2017.00131. PMID: 29375326; PMCID: PMC5767177.
27. Kipanyula MJ, Sife AS. Global Trends in Application of Stereology as a Quantitative Tool in Biomedical Research. *Biomed Res Int*. (2018) Sep 13;2018:1825697. doi: 10.1155/2018/1825697. PMID: 30302337; PMCID: PMC6158933.
28. Sethi MK, Zaia J. Extracellular matrix proteomics in schizophrenia and Alzheimer's disease. *Anal Bioanal Chem*. (2017) Jan;409(2):379-394. doi: 10.1007/s00216-016-9900-6. Epub 2016 Sep 6. PMID: 27601046; PMCID: PMC5203946.
29. Bhuiyan P, Sun Z, Khan MA, Hossain MA, Rahman MH, Qian Y. System biology approaches to identify hub genes linked with ECM organization and inflammatory signaling pathways in schizophrenia pathogenesis. *Heliyon*. (2024) Jan 26;10(3):e25191. doi: 10.1016/j.heliyon.2024.e25191. PMID: 38322840; PMCID: PMC10844262.
30. Ahmadpour, S., Behrad, A., Vega, I. Dark Neurons: A protective mechanism or a mode of death. *JMH*, (2019); 3(2): 125-131. doi: 10.21608/jmh.2020.40221.1081
31. Rey, Federica^{1,2}; Ottolenghi, Sara³; Zuccotti, Gian Vincenzo^{1,2,4}; Samaja, Michele³; Carelli, Stephana PhD^{1,2,*}. Mitochondrial dysfunctions in neurodegenerative diseases: role in disease pathogenesis, strategies for analysis and therapeutic prospects. *Neural Regeneration Research* (2022)17(4):p 754-758, April. | DOI: 10.4103/1673-5374.322430

32. Roberts RC. Mitochondrial dysfunction in schizophrenia: With a focus on postmortem studies. *Mitochondrion*. (2021) Jan;56:91-101. doi: 10.1016/j.mito.2020.11.009. Epub 2020 Nov 20. PMID: 33221354; PMCID: PMC7810242.
33. Roberts RC. Postmortem studies on mitochondria in schizophrenia. *Schizophr Res*. (2017) Sep;187:17-25. doi: 10.1016/j.schres.2017.01.056. Epub 2017 Feb 9. PMID: 28189530; PMCID: PMC5550365.
34. Kathuria A, Lopez-Lengowski K, McPhie D, Cohen BM, Karmacharya R. Disease-specific differences in gene expression, mitochondrial function and mitochondria-endoplasmic reticulum interactions in iPSC-derived cerebral organoids and cortical neurons in schizophrenia and bipolar disorder. *Discov Ment Health*. (2023);3(1):8. doi: 10.1007/s44192-023-00031-8. Epub 2023 Mar 9. PMID: 36915374; PMCID: PMC9998323.
35. Wang J, Fröhlich H, Torres FB, Silva RL, Poschet G, Agarwal A, Rappold GA. Mitochondrial dysfunction and oxidative stress contribute to cognitive and motor impairment in FOXP1 syndrome. *Proc Natl Acad Sci U S A*. (2022) Feb 22;119(8):e2112852119. doi: 10.1073/pnas.2112852119. PMID: 35165191; PMCID: PMC8872729.
36. Rival T, Soustelle L, Strambi C, Besson MT, Iché M, Birman S. Decreasing glutamate buffering capacity triggers oxidative stress and neuropil degeneration in the *Drosophila* brain. *Curr Biol*. (2004) Apr 6;14(7):599-605. doi: 10.1016/j.cub.2004.03.039. PMID: 15062101.
37. Zhang JY, Liu TH, He Y, Pan HQ, Zhang WH, Yin XP, Tian XL, Li BM, Wang XD, Holmes A, Yuan TF, Pan BX. Chronic Stress Remodels Synapses in an Amygdala Circuit-Specific Manner. *Biol Psychiatry*. (2019) Feb 1;85(3):189-201. doi: 10.1016/j.biopsych.2018.06.019. Epub 2018 Jul 5. PMID: 30060908; PMCID: PMC6747699.
38. Falkai P, Rossner MJ, Raabe FJ, Wagner E, Keeser D, Maurus I, Roell L, Chang E, Seitz-Holland J, Schulze TG, Schmitt A. Disturbed Oligodendroglial Maturation Causes Cognitive Dysfunction in Schizophrenia: A New Hypothesis. *Schizophr Bull*. (2023) Nov 29;49(6):1614-1624. doi: 10.1093/schbul/sbad065. PMID: 37163675; PMCID: PMC10686333.
39. Schmitt A, Tatsch L, Vollhardt A, *et al.* Decreased Oligodendrocyte Number in Hippocampal Subfield CA4 in Schizophrenia: A Replication Study. *Cells*. (2022);11(20):3242. Published 2022 Oct 15. doi:10.3390/cells11203242
40. Rigg N, Abu-Hijleh FA, Patel V, Mishra RK. Ketamine-induced neurotoxicity is mediated through endoplasmic reticulum stress *in vitro* in STHdhQ7/Q7 cells. *Neurotoxicology*. (2022) Jul;91:321-328. doi: 10.1016/j.neuro.2022.06.004. Epub 2022 Jun 18. PMID: 35728656.
41. Choudhury D, Autry AE, Tolias KF, Krishnan V. Ketamine: Neuroprotective or Neurotoxic? *Front Neurosci*. (2021) Sep 10;15:672526. doi: 10.3389/fnins.2021.672526. PMID: 34566558; PMCID: PMC8461018.
42. Dreier JP, Isele T, Reiffurth C, Offenhauser N, Kirov SA, Dahlem MA, Herreras O. Is spreading depolarization characterized by an abrupt, massive release of Gibbs free energy from the human brain cortex? *Neuroscientist*. (2013) Feb;19(1):25-42. doi: 10.1177/1073858412453340. Epub 2012 Jul 24. PMID: 22829393; PMCID: PMC3526686.
43. Forsyth JK, Lewis DA. Mapping the Consequences of Impaired Synaptic Plasticity in Schizophrenia through Development: An Integrative Model for Diverse Clinical Features. *Trends Cogn Sci*. (2017) Oct;21(10):760-778. doi: 10.1016/j.tics.2017.06.006. Epub 2017 Jul 25. PMID: 28754595; PMCID: PMC5610626.
44. Song I, Dityatev A. Crosstalk between glia, extracellular matrix and neurons. *Brain Res Bull*. (2018) Jan;136:101-108. doi: 10.1016/j.brainresbull.2017.03.003. Epub 2017 Mar 8. PMID: 28284900.
45. Ahmadpour S. Synaptic microenvironment and altered state of consciousness in schizophrenia: a possible link between synapse geometry and orchestrated objective reduction theory. *Egypt J Neurol Psychiatry Neurosurg* 59, 117 (2023). <https://doi.org/10.1186/s41983-023-00719-2>
-

الملخص العربي

تأثيرات نموذج نقص وظيفة N-ميثيل-D-أسبارتات للفصام المُحفَّز بالكيثامين على نيوربييل الحصين: تحليل مجهر إلكتروني مجسم ونافذ

شهريار أحمد بور^{١،٢}، محمد أمين فرقاني^٢، أمير حسين نجمي^٢، مائدة أميري شهري^٢، شايان زنجانيان^٢، مهدي نوري^٢

^١مركز تعليم وبحوث علوم الأعصاب، قسم التشريح، كلية الطب، جامعة شمال خراسان للعلوم الطبية

^٢جامعة شمال خراسان للعلوم الطبية. بجنورد، إيران

الخلفية: يُعدّ النيوربييل شبكةً كثيفةً بين العناصر العصبية الدبقية، ويشارك في العديد من الأنشطة، مثل الوظائف الإدراكية. وقد لوحظ تأثير النيوربييل في الاضطرابات العصبية. الفصام حالةٌ صحيةٌ عقليةٌ تُعرّف بانخفاض في الوظائف الإدراكية. يُعدّ الحصين البنية الرئيسية للجهاز الحوفي، ويُنظّم الوظائف الإدراكية.

الهدف من العمل: دراسة الآثار المحتملة للفصام على النيوربييل في الحصين.

المواد والطرق: استُخدم في هذه الدراسة ثلاثون جرداً ذكراً من فئران ويستار. صُنِّفت الجرذان إلى ثلاث مجموعاتٍ مُتميّزة (عددها ١٠ لكل مجموعة)، وهي: الكيثامين، والمحلّط الملحي الطبيعي (١ مل، داخل الصفاق) (مجموعة وهمية)، ومجموعات الضبط. عُولجت مجموعة الكيثامين بالكيثامين (١٠ ملجم/كجم، داخل الصفاق) لمدة سبعة أيام. أما المجموعة الوهمية، فقد تلقت محلّطاً ملحيّاً طبيعياً (١ مل، داخل الصفاق) فقط. بعد أسبوع واحد، أُزيلت الأدمغة، وُعُولجت المقاطع لإجراء دراسة نسيجية. قُيس سطح النيوربييل بطريقة التجسيم. واستُخدمت دراسة المجهر الإلكتروني النافذ (TEM) لدراسة التغيرات فوق البنيوية.

النتائج: على عكس المجموعتين الوهمية والضابطة، لوحظت زيادة ملحوظة في مساحات أسطح CA^٤ و CA^٣ و CA^١ في مرضى الفصام ($P=0.006$). كما أظهر عدد الخلايا العصبية المتدهورة في مناطق قرن الأمون زيادة ملحوظة ($P=0.001$). كشفت نتائج المجهر الإلكتروني النافذ عن مجموعة واسعة من التغيرات فوق البنيوية، بما في ذلك الخلايا العصبية المظلمة، واضطراب الفراغات خارج الخلوية، وتلف الميالين، وتنكس الميتوكوندريا في مجموعة مرضى الفصام.

الخلاصة: يؤدي الفصام إلى توسع النيوربييل في المناطق الفرعية CA. ويرتبط توسع النيوربييل بتغيرات فوق بنيوية، بما في ذلك تنكس الميتوكوندريا، وتلف المحور العصبي، وتنكس الخلايا العصبية. الكلمات المفتاحية: نيوروبييل، الفصام، الحصين